A mouse model for human short-stature syndromes identifies *Shox2* as an upstream regulator of *Runx2* during long-bone development

John Cobb*, Andrée Dierich†, Yolande Huss-Garcia†, and Denis Duboule*‡

*Department of Zoology and Animal Biology and National Research Center ''Frontiers in Genetics,'' Sciences III, University of Geneva, Quai Ernest Ansermet 30, 1211 Geneva 4, Switzerland; and †Institut de Génétique et de Biologie Moléculaire et Cellulaire/Institut Clinique de la Souris, Centre National de la Recherche Scientifique/Institut National de la Santé et de la Recherche Médicale/Université Louis Pasteur/Collège de France, BP 10142, 67404 Strasbourg, France

Edited by Pierre Chambon, Institut de Génétique et de Biologie Moléculaire, Strasbourg, France, and approved January 11, 2006 (received for review December 7, 2005)

Deficiencies or mutations in the human pseudoautosomal *SHOX* gene are associated with a series of short-stature conditions, including Turner syndrome, Leri–Weill dyschondrosteosis, and Langer mesomelic dysplasia. Although this gene is absent from the mouse genome, the closely related paralogous gene *Shox2* displays a similar expression pattern in developing limbs. Here, we report that the conditional inactivation of *Shox2* in developing appendages leads to a strong phenotype, similar to the human conditions, although it affects a different proximodistal limb segment. Furthermore, using this mouse model, we establish the cellular etiology of these defects and show that *Shox2* acts upstream the *Runx2* gene, a key regulator of chondrogenesis.

limb | *SHOX*

The human pseudoautosomal gene *SHOX* was initially identified as a candidate gene for the short-stature phenotype associated with Turner syndrome (1, 2). Whereas the contribution of *SHOX* to the abnormal phenotype in Turner patients is clearly due to haploinsufficiency, the function of *SHOX* is more apparent in Langer syndrome, which is caused by a complete lack of *SHOX* function (3). Langer patients have extremely short and bowed arm and leg zeugopod elements, the radius/ulna and tibia/fibula, respectively. The developmental basis for these short limbs is unclear because of the paucity of data from *SHOX*-mutant human embryos. However, abnormal and disordered chondrocytes were reported in the growth plates of patients with Leri–Weill dyschondrosteosis, which is caused by a heterozygous *SHOX* mutation (4). Immunohistochemical staining showed that the SHOX protein is expressed in growth-plate chondrocytes, leading to the proposal that the *SHOX* product normally functions to repress chondrocyte differentiation and hypertrophy (5). In this view, the short limbs of *SHOX*-deficient patients would derive from precocious chondrocyte differentiation leading to premature growth-plate fusion.

Mice have lost their *Shox* gene, along with other pseudoautosomal genes, during evolution (6). However, rodents do retain the autosomal *Shox2* paralog, which is also found in humans. Murine SHOX2 protein is almost identical to human SHOX2 (99% amino acid identity) and is also highly similar to human SHOX (79%, with an identical DNA-binding homeodomain) (7). Furthermore, human *SHOX* and *SHOX2* and murine *Shox2* are highly expressed in the proximal domains of developing limbs. Clement-Jones *et al.* (7) compared the *SHOX* with the *SHOX2* expression domain in human embryonic limbs [at Carnegie Stage 18, i.e., the equivalent to murine embryonic day 12.5 (E12.5)] and found that *SHOX2* is expressed more proximally than *SHOX*, whose transcripts are detected in the middle part of the limb, in agreement with the phenotype of *SHOX*-deficient humans. Likewise, mouse *Shox2* is expressed in the proximal limb. However, its expression at E12.5 extends from the body wall up to the hand plate (8), from which it is excluded, thus recapitulating the expression of both human *SHOX* and *SHOX2* and further suggesting that it displays a function in developing limbs related to that of its two human counterparts.

We identified *Shox2* as a candidate target gene of HOXD proteins in developing distal limbs by using a microarray screen (9). *Shox2* appeared up-regulated in the presumptive digit domain after deletion of the *Hoxd* gene cluster, indicating a potential repressive effect of *Hoxd* genes on *Shox2* transcription in distal limbs. These results suggested that *Shox2* could be involved in patterning more proximal limb elements. We investigated this issue by producing mice in which the *Shox2* gene was conditionally deleted in developing limbs.

Results and Discussion

We flanked the entire coding region of *Shox2* with *LoxP* sites (10), such as to induce deletion upon exposure to the Cre recombinase (Fig. 1). Mice carrying such a floxed allele as well as a fully deleted copy and the limb-specific *Prx1-Cre* transgene (11) (hereafter referred to as $Shox2^{c/-}$) were thus devoid of any *Shox2* transcript in their developing limbs (Fig. 1 *b* and *c*). This strategy allowed us to bypass the lethality caused by homozygous germ line deletion of *Shox2* (12), occurring at around E12.5 from an apparent circulatory defect (data not shown), thus precluding the observation of the limb phenotype. The lethal phenotype caused by the *Shox2* inactivation may explain why no *SHOX2*-associated phenotype has ever been described in humans.

Shox2 conditional mutant mice were born in the expected Mendelian ratios. Unlike human *SHOX* patients, heterozygous mutant mice had no obvious abnormal limb phenotype. In contrast, homozygous mutants had markedly shortened limbs. Despite their short stature, $Shox2^{c/-}$ mice could survive to adulthood as long as food and water were made accessible. Surprisingly, skeletal preparations of newborn and adult skeletons revealed that limb shortening was due to the virtual absence of the humerus and femur (the stylopod elements; Fig. 2). At birth the only bone visible in either stylopod was an abnormal piece of dorsal humerus that did not span the axis of the limb (Fig. 2*a*). The femur was even more severely affected, because no ossification was apparent in the tiny femoral cartilage anlage (Fig. 2*b*). By adulthood the humeral and femoral cartilages had eventually ossified, but little bone growth occurred (Fig. 2 *c* and *d*). In contrast to the zeugopod phenotype caused by human *SHOX* mutations, the radius and ulna of $Shox2^{c/-}$ mice were not

Conflict of interest statement: No conflicts declared.

This paper was submitted directly (Track II) to the PNAS office.

Abbreviation: E*n*, embryonic day *n*.

‡To whom correspondence should be addressed. E-mail: Denis.Duboule@zoo.unige.ch.

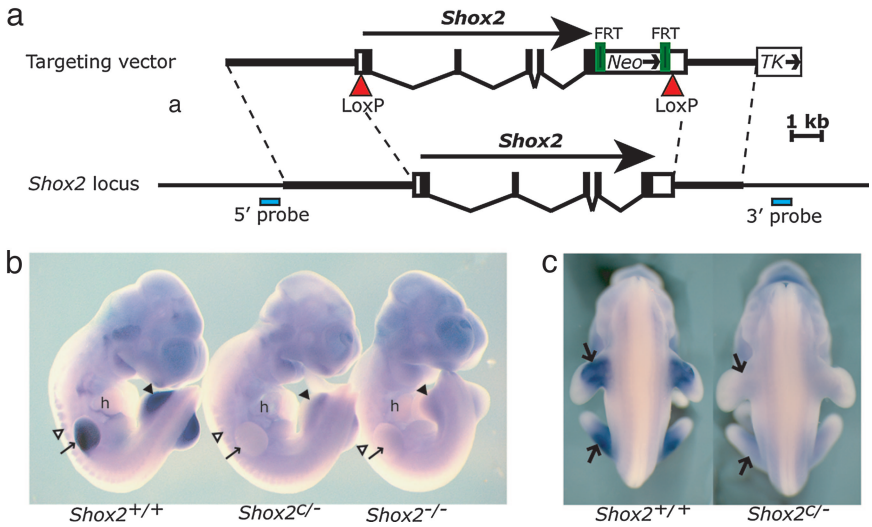

Fig. 1. Conditional deletion of the *Shox2* gene in limbs. (*a*) Diagram of both the recombination vector (*Upper*) and the *Shox2* locus targeted by homologous recombination (*Lower*). *Lox*P sites were introduced flanking the *Shox2* coding region such that Cre recombinase deletes the entire sequence. Rectangles represent the five *Shox2* exons with filled regions showing the coding sequence. The position of external probes is indicated by blue boxes. (*b*) *In situ* hybridization with a *Shox2* riboprobe of E10.5 littermates produced from mice carrying targeted *Shox2* alleles. In the embryo carrying one floxed and one germ line-deleted *Shox2* allele and the *Prx1-Cre* transgene (abbreviated hereafter as $Shox2^{c/-}$), *Shox2* expression is specifically removed from both forelimb (arrow) and hindlimb (▲) buds. Expression is still detected in the heart (h), dorsal root ganglia (△), pharyngeal arches, and the face of the conditional mutant, although it is reduced when compared with wild-type littermates ($Shox2^{+/+}$). The embryo carrying two germ line-deleted alleles ($Shox2^{-/-}$) serves as a control for background staining. (*c*) *Shox2 in situ* hybridization of E11.5 embryos. At this stage, *Shox2* expression is restricted to the proximal domain of the limbs (arrows) in the wild-type embryos but is not detected in the limbs of the *Prx1-Cre* conditional mutant littermate ($Shox2^{c/-}$).

significantly shorter than those of wild-type littermates. However, the hindlimb zeugopod of $Shox2^{c/-}$ mice was clearly shorter, and the tibia showed marked bowing, reminiscent of the tibial phenotype caused by *SHOX* haploinsufficiency (13). Although the limb elements mostly affected in $Shox2^{c/-}$ mice are more proximal than those in human *SHOX* patients, the type of alteration, a drastic shortening of long bones, is remarkably similar, making this mouse model suitable for understanding the human pathology.

We sought to determine when and how the *Shox2*-mutant phenotype appears. Limb bones are formed by endochondral ossification, whereby a cartilage model is replaced by bone later in embryonic development. Therefore, the deletion of *Shox2* could affect either chondrocyte differentiation or the subsequent ossification of cartilage models. We stained the cartilage models in E12.5 limbs, i.e., right after their appearance (Fig. 3*a*), and observed, already at this early stage, a significant shortening of the humerus and femur cartilages (≈50% shorter than those

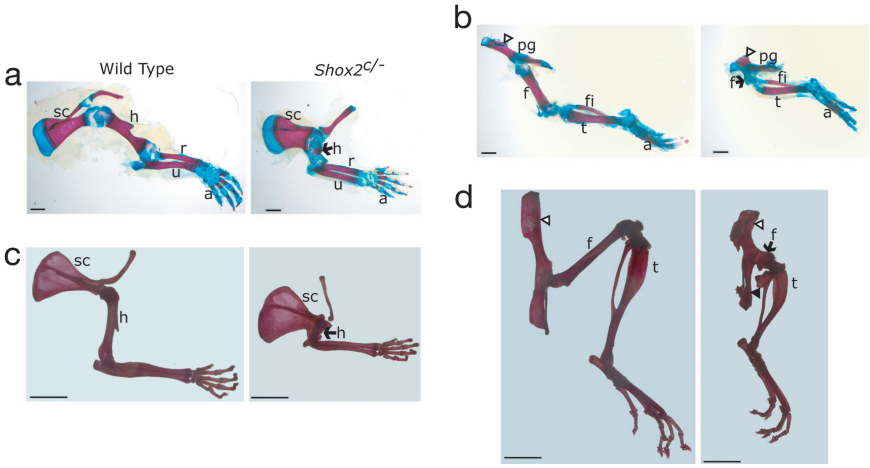

Fig. 2. Phenotype of *Shox2* conditional mutants in limbs. (*a*) Newborn forelimb skeletons (blue, cartilage; red, bone). The humerus in the mutant forelimb is virtually absent except for a small ossification center (arrow), which is located on the anterior/dorsal surface of the cartilage and does not span the axis of the limb. The rest of the limb is relatively normal, except for a slight broadening of the distal scapula (sc). r, radius; u, ulna; a, autopod. (*b*) Hindlimbs of newborn animals. The femur (f) in the mutant is represented only by a small cartilaginous extension (arrow) of the pelvic girdle (pg). The tibia (t) and fibula (fi) are also noticeably shorter in the mutant, whereas the autopod (paw) is normal. The ilium (△) is also small in the mutant and contains an abnormal asymmetric ossification center similar to that of the humerus in *a*. (*c*) Adult forelimb skeletons with bones stained with Alizarin red. The extremely small humerus (h) of the mutant is ossified and fused to the scapula (sc). (*d*) Adult hindlimbs. The tiny mutant femur (f) is now ossified and fused to the pelvic girdle. The tibia (t) is short and bowed, and the fibula contains an ectopic ossification center (▲). As in newborns, the ilium (△) is significantly shorter in the mutant. In contrast, the mutant autopod is of similar size and morphology to that of control animals. [Scale bar: 1 mm (*a* and *b*) and 5 mm (*c* and *d*).]

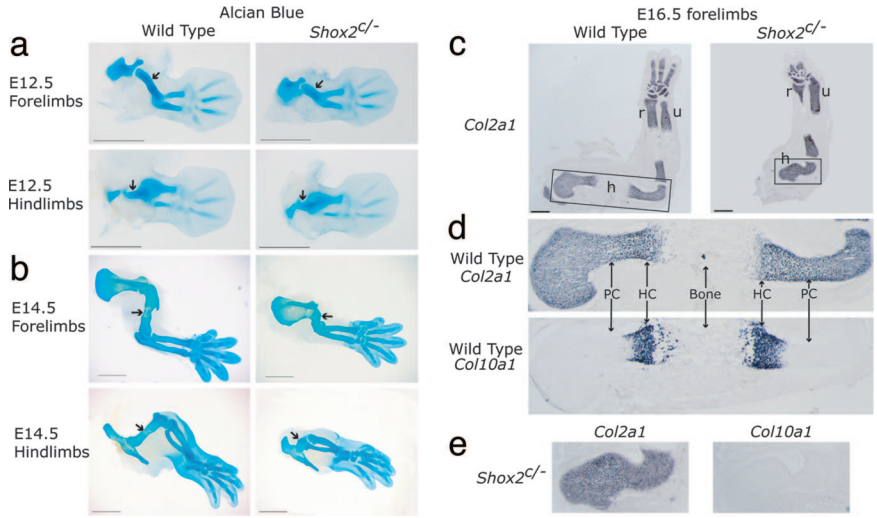

Fig. 3. In *Shox2*-mutant embryos the cartilaginous templates for the stylopod elements are smaller and contain only immature chondrocytes. (*a*) At E12.5, the cartilage model of the humerus (arrow) is approximately twice as long in wild-type as compared with mutant embryos. Similarly, the cartilage of the presumptive femur (arrow) is reduced in E12.5 mutant hindlimbs. (*b*) At E14.5, mutant limbs have an abnormal small humerus and femur (arrows) approximately as severe as that observed in newborn and adult mutant animals (compare with Fig. 2). (Scale bar: 1 mm.) (*c*) Longitudinal sections from E16.5 forelimbs stained with a *Col2a1* riboprobe. Boxes indicate magnified regions shown in *d* and *e*. The small mutant humerus (h) is filled with immature chondrocytes expressing *Col2a1*, whereas the wild-type limb has *Col2a1*-positive chondrocytes at either end of the humerus. The middle of the wild-type bone is *Col2a1*-negative where chondrocytes have matured and bone is forming. r, radius; u, ulna. (Scale bar: 0.5 mm.) (*d*) Magnified view of the wild-type humerus from *c* and an adjacent section stained with a *Col10a1* riboprobe [a marker for hypertrophic chondrocytes (HC)]. Arrows indicate the position of bone and chondrocyte populations that are progressively more differentiated toward the middle of the humerus [proliferating chondrocytes (PC)]. (*e*) Magnified view of the $Shox2^{c/-}$ humerus from *c* (at the same scale as in *d*) and an adjacent section stained with a *Col10a1* riboprobe. The mutant humerus contains only *Col2a1*-expressing chondrocytes that are negative for *Col10a1*.

of the controls). By E14.5, just as ossification was beginning, the phenotype had fully developed and was as severe as in newborns (Fig. 3*b*). This result indicated that the *Shox2*-mutant defect was caused by abnormal chondrocyte maturation (for example, by precocious or delayed chondrocyte differentiation) rather than by abnormal bone formation *per se*. Because immature cells that have just entered the chondrocytic lineage express *Col2a1*, we assessed the transcription of this marker in $Shox2^{c/-}$ chondrocytes. Sections of E16.5 limbs revealed that the $Shox2^{c/-}$ humerus was filled with immature *Col2a1*-positive cells at a time when bone formation is normally well underway (Fig. 3 *c–e*).

Chondrocyte proliferation and normal differentiation depend on *Indian hedgehog* (*Ihh*) signaling (14); *Ihh* is expressed in nondividing prehypertrophic chondrocytes. The subsequent transformation of these cells into mature hypertrophic chondrocytes is accompanied by the expression of the *Col10a1* marker gene. We stained sections of E14.5–E18.5 limbs for the presence of these two markers. From E14.5 to E16.5, the $Shox2^{c/-}$ mutant humerus had little detectable *Ihh* (data not shown) and no *Col10a1* signal (Fig. 3*e*), unlike in controls, indicating a severe delay in chondrocyte differentiation. Even as late as E18.5, most mutant chondrocytes still expressed the early marker *Col2a1*, whereas the wild-type humerus displayed *Col2a1*-positive cells only at either end of the bone (Fig. 4). Likewise, the mutant femur at E18.5 contained only *Col2a1*-positive cells, whereas the expected *Col10a1* staining was absent (data not shown). Hypertrophic chondrocytes eventually appeared in the mutant humerus, although in an abnormal asymmetric location, making the formation of a growth plate impossible (Fig. 4*c*), in contrast to control bones where such cells appeared in a zone spanning the long axis of the bone (Fig. 4*a*) that makes longitudinal growth possible.

These results showed that *Shox2*-mutant limb bones are severely delayed in their process of chondrocyte differentiation. This defect is more severe than that observed in *Ihh*-null mice, in which *Col10a1* expression is detected by E13.5 and, accordingly, hypertrophy is present by E14.5 (14). Therefore, the disruption of the chondrocyte differentiation process in *Shox2* mutants lies somewhere between the activation of *Col2a1* and *Ihh* transcription. Gene members of the *Runx* family have recently been shown to control chondrocyte hypertrophy. Mice lacking *Runx2/Runx3* functions have a complete lack of chondrocyte differentiation beyond the *Col2a1* stage, and *Runx2* was shown to directly regulate *Ihh* expression (15). Interestingly, a lack of *Runx2* function is sufficient to eliminate chondrocyte hypertrophy in the humerus and femur (16), whereas both *Runx2* and *Runx3* functions must be removed to block hypertrophy in the more distal elements (15). Therefore, we looked at *Runx2*

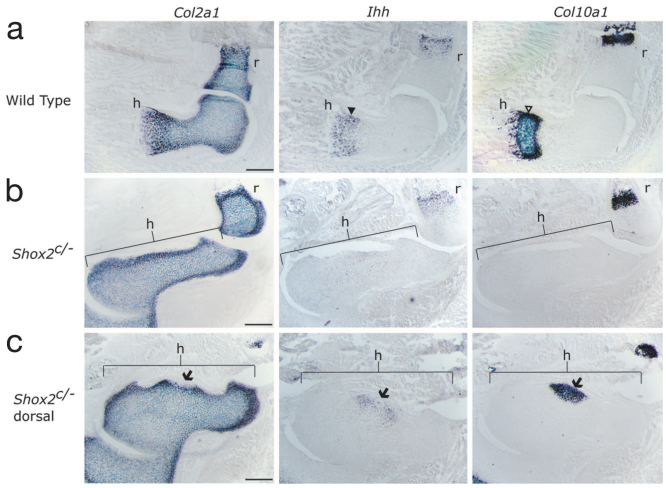

Fig. 4. Chondrocyte hypertrophy is severely delayed and abnormal in the *Shox2*-mutant humerus. Serial longitudinal sections from E18.5 forelimbs hybridized with *Col2a1*, *Ihh*, and *Col10a1* riboprobes. (*a*) As in Fig. 3 *c* and *d*, *Col2a1*-positive chondrocytes are found at the distal end of the wild-type humerus (h). Toward the middle of the bone, *Ihh* expression is present in a band of prehypertrophic chondrocytes (▲) that overlaps with a zone of hypertrophic chondrocytes (△) positive for *Col10a1*. (*b*) In contrast, in longitudinal sections through the center of the mutant humerus, there are few prehypertrophic (*Ihh*-positive) and no hypertrophic (*Col10a1*-positive) chondrocytes. Instead, the length of the humerus (bracket) is filled with uniformly small, *Col2a1*-positive chondrocytes. The mutant radius (r) shows the same zones of chondrocytes present in the wild-type sections. (*c*) Sections through the same humerus as in *b* but located ≈100 μm more dorsally. Hypertrophy was first detected in the mutant humerus as a cluster of *Ihh* and *Col10a1*-expressing cells at E18.5 (arrow) that are approximately in the same position as the abnormal ossification of the humerus seen in newborn $Shox2^{c/-}$ mice (Fig. 2*a*). The hypertrophic cells in the $Shox2^{c/-}$ humerus are delayed in their appearance but are also abnormal in their location and shape as a cluster displaced from the center of the bone. Wild-type hypertrophic cells are found as a zone of cells that is perpendicular to and spans the long axis of the bone (e.g., △ in *a*). (Scale bar: 250 μm.)

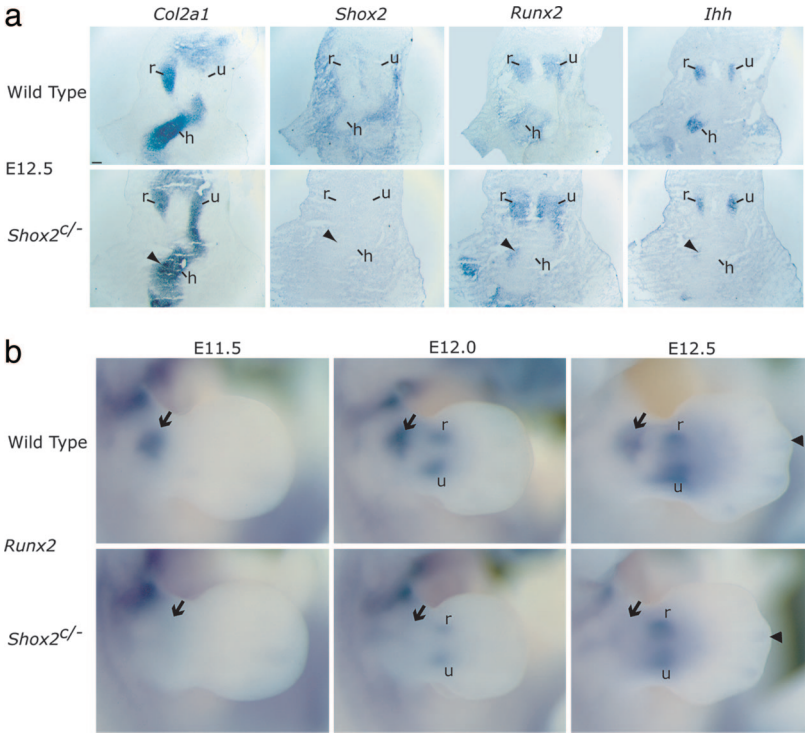

Fig. 5. The expression of *Ihh* and its activator *Runx2* is severely reduced from the beginning of chondrocyte differentiation. (*a*) Serial longitudinal sections from E12.5 forelimbs stained with *Col2a1*, *Shox2*, *Runx2*, and *Ihh* riboprobes. *Col2a1* expression reveals the location of immature chondrocytes of the cartilaginous condensations that will form the radius (r), ulna (u), and humerus (h). *Shox2* expression is seen only in the wild-type forelimb and most abundantly there in the tissue surrounding the condensations but is also weakly detected in chondrocytes in the center of the wild-type humerus. In the mutant, *Runx2* and *Ihh* staining is mostly absent from the humerus and visible only in the anterior periphery of the condensation (arrowheads). In the control limb, *Ihh* is expressed in the center of the humerus condensation and is surrounded by a domain of *Runx2* expression that is in turn within an area of *Shox2* expression. (Scale bar: 100 μm.) (*b*) Whole-mount *in situ* hybridization with a *Runx2* riboprobe. *Runx2* expression appears in the presumptive humerus domain (arrow) at E11.5 in wild-type embryos. During day 12 of development, *Runx2* expression is activated in the domains of the presumptive radius (r) and ulna (u) (E12.0) and then begins to appear in digits (▲) at E12.5. In contrast, in *Shox2*-mutant limbs, *Runx2* expression is not visible through E12.5 in the humerus domain (arrows), even though the radius, ulna, and digit expression is activated with the same kinetics as that in wild-type limbs.

expression in $Shox2^{c/-}$ mice, and, strikingly, very few *Runx2*-positive cells were scored in the humerus at E12.5 (Fig. 5*a*). A few positive cells were detected at the periphery of the humerus, in the same location where hypertrophic chondrocytes were seen at E18.5. The absence of *Runx2* expression was further assessed by whole mount *in situ* hybridization at E11.5, when the humerus condensation is just forming (Fig. 5*b*). Significantly, the normal proximal expression domain corresponding to the humerus cartilage model was virtually absent from mutant limb buds (Fig. 5*b*, arrow).

Interestingly, limb bones of developing *Runx2*/*Runx3*-null mice are affected in much the same way as the $Shox2^{c/-}$ humerus and femur (15). From this and the above-mentioned results, we propose that alteration in *Runx2* expression is responsible for the abnormal limb phenotypes of human *SHOX* patients, via a defect in chondrocyte differentiation. A delayed and eventual asymmetric differentiation of chondrocytes would explain both the small zeugopod bones and their curvatures (e.g., Madelung's deformity) observed in people with *SHOX* deficiencies. In this view, human SHOX and SHOX2 may have similar functions, but at different proximodistal positions. It is particularly significant that *Shox2* is the first gene shown to be necessary to form both the humerus and femur but not the distal limb, a role in patterning the stylopod that was assumed to be a function of *Hox* genes (17). *Hox* genes alone are not sufficient to pattern the forelimbs, because in the absence of *Hox* function in limbs a sizeable fragment of the humerus develops (18), perhaps reflecting a comparable function of *Shox2* in this region. Furthermore, the *Shox2*-mutant phenotype is apparently not due to changes in *Hox* gene expression, because we observed no substantial changes in the expression of *Hoxd9*, *Hoxd10*, *Hoxd11*, *Hoxd13*, or *Hoxa11* in $Shox2^{c/-}$ mutant embryos from E9.5 to E12.5 (data not shown). Noteworthy, the double knockout of *Hoxa11*/*Hoxd11* showed a cellular phenotype in both radius and ulna very similar to that described here for the *Shox2*-mutant humerus (19). Although the authors of that study did not examine *Runx2* expression, they did report a lack of *Ihh* and *Col10a1* expression and a severe delay of chondrocyte differentiation in the affected elements that could be due to a failure to activate *Runx2* in the zeugopod.

Runx2 is a particularly attractive candidate as a hub for regulatory inputs that converge to control chondrocyte differentiation and bone formation. The histone deacetylase HDAC4 has been shown to control chondrocyte hypertrophy by inhibiting both the transcription and activity of *Runx2* (20), and, recently, Hill *et al.* (21) showed that *Wnt* signaling controls *Runx2* expression in the developing limb. Our identification of *Shox2* as a stylopod-specific regulator of *Runx2* expression in mice implies that different transcription factors act upstream of *Runx2* at different locations along the limb's proximodistal axis, which may introduce morphogenetic flexibility, in particular in an evolutionary context, and thus could account for the variability in the relative lengths of long bones observed amongst different tetrapods. Therefore, it will be interesting to determine which other genes are necessary for *Runx2* activation in more distal limb domains such as digits. Finally, although we have identified a candidate cellular and molecular mechanism for the bone defect in humans carrying *SHOX*-deficiency, future studies must elucidate why these similar alterations affect different parts of the appendages in human and mice.

Materials and Methods

Gene Targeting. Mouse BAC RP23-103D17 containing the *Shox2* gene was obtained from Children's Hospital Oakland Research Institute (Oakland, CA). A 15.7-kb fragment containing the *Shox2* gene was subcloned from the BAC by gap repair as described (10). *LoxP* sites were introduced 160 bp upstream of the start codon of *Shox2* and 315 bp downstream of the stop codon by recombineering techniques with plasmids, which were a gift from N. Copeland (National Cancer Institute, Frederick, MD), using reported technology (10). The targeting construct was electroporated into ES cell line P1 (derived from mouse strain 129S2/SvPas). Electroporation and ES cell culture were as described (22). ES cell clones were screened for homologous recombination by long-range PCR (Roche) and then verified for correct targeting by Southern blotting with 5′ and 3′ external

probes. Four positive ES clones were identified, and two were injected into C57BL/6 blastocysts according to standard techniques. Resulting chimeras transmitted the floxed allele as verified by Southern blotting. The neomycin selection cassette was removed from the genome of mice carrying the floxed allele by breeding to *FLPe* mice (23). The conditional allele was derived from these mice bred to males carrying one germ line-deleted *Shox2* allele and expressing Cre recombinase under control of the *Prx1* promoter (*Prx1-Cre*) (11). The germ line-deleted allele was obtained by passing the floxed allele through the germ line of female *Prx1-Cre* mice. All mice were genotyped by PCR.

***In Situ* Hybridization, Probes, and Skeletal Analysis.** *In situ* hybridization on 10-μm cryosections was performed according to the Eumorphia standard operating procedure (24). Whole-mount *in situ* hybridization using embryos fixed in 4% paraformaldehyde was performed according to standard procedures. The *Shox2* riboprobe was described previously (9). The *Col2a1* probe was a gift from B. Olsen (Harvard Medical School, Boston), and the *Ihh* and *Col10a1* probes were gifts from A. Vortkamp (Universitaet Duisburg-Essen, Germany). cDNA for the *Runx2* probe was generated by RT-PCR as described (25). Skeletal staining with Alizarin red and Alcian blue and fetal cartilage staining with Alcian blue were done with established techniques. At least two replicates were performed for each reported condition, and a representative staining is shown.

We are grateful to P. Chambon for consultations; N. Fraudeau for technical assistance; M. Kmita, M. McDonald, N. Soshnikova, and F. Spitz for sharing reagents and discussions; M. Logan, S. Dymecki, and D. Metzger for mice; A. Vortkamp and B. Olsen for probes; and N. Copeland for recombineering plasmids. This work was supported by funds from the Canton de Genève, the Louis-Jeantet Foundation, the Swiss National Research Fund, the National Center for Competence in Research (NCCR) "Frontiers in Genetics," and the European Union program "Eumorphia."

1. Rao, E., Weiss, B., Fukami, M., Rump, A., Niesler, B., Mertz, A., Muroya, K., Binder, G., Kirsch, S., Winkelmann, M., *et al.* (1997) *Nat. Genet.* **16,** 54–63.
2. Ellison, J. W., Wardak, Z., Young, M. F., Gehron Robey, P., Laig-Webster, M. & Chiong, W. (1997) *Hum. Mol. Genet.* **6,** 1341–1347.
3. Zinn, A. R., Wei, F., Zhang, L., Elder, F. F., Scott, C. I., Jr., Marttila, P. & Ross, J. L. (2002) *Am. J. Med. Genet.* **110,** 158–163.
4. Munns, C. F., Glass, I. A., LaBrom, R., Hayes, M., Flanagan, S., Berry, M., Hyland, V. J., Batch, J. A., Philips, G. E. & Vickers, D. (2001) *Hand Surg.* **6,** 13–23.
5. Munns, C. J., Haase, H. R., Crowther, L. M., Hayes, M. T., Blaschke, R., Rappold, G., Glass, I. A. & Batch, J. A. (2004) *J. Clin. Endocrinol. Metab.* **89,** 4130–4135.
6. Gianfrancesco, F., Sanges, R., Esposito, T., Tempesta, S., Rao, E., Rappold, G., Archidiacono, N., Graves, J. A., Forabosco, A. & D'Urso, M. (2001) *Genome Res.* **11,** 2095–2100.
7. Clement-Jones, M., Schiller, S., Rao, E., Blaschke, R. J., Zuniga, A., Zeller, R., Robson, S. C., Binder, G., Glass, I., Strachan, T., *et al.* (2000) *Hum. Mol. Genet.* **9,** 695–702.
8. Semina, E. V., Reiter, R. S. & Murray, J. C. (1998) *Hum. Mol. Genet.* **7,** 415–422.
9. Cobb, J. & Duboule, D. (2005) *Development (Cambridge, U.K.)* **132,** 3055–3067.
10. Liu, P., Jenkins, N. A. & Copeland, N. G. (2003) *Genome Res* **13,** 476–484.
11. Logan, M., Martin, J. F., Nagy, A., Lobe, C., Olson, E. N. & Tabin, C. J. (2002) *Genesis* **33,** 77–80.
12. Yu, L., Gu, S., Alappat, S., Song, Y., Yan, M., Zhang, X., Zhang, G., Jiang, Y., Zhang, Z., Zhang, Y. & Chen, Y. (2005) *Development (Cambridge, U.K.)* **132,** 4397–4406.
13. Ross, J. L., Kowal, K., Quigley, C. A., Blum, W. F., Cutler, G. B., Jr., Crowe, B., Hovanes, K., Elder, F. F. & Zinn, A. R. (2005) *J. Pediatr.* **147,** 499–507.
14. St-Jacques, B., Hammerschmidt, M. & McMahon, A. P. (1999) *Genes Dev.* **13,** 2072–2086.
15. Yoshida, C. A., Yamamoto, H., Fujita, T., Furuichi, T., Ito, K., Inoue, K., Yamana, K., Zanma, A., Takada, K., Ito, Y. & Komori, T. (2004) *Genes Dev.* **18,** 952–963.
16. Inada, M., Yasui, T., Nomura, S., Miyake, S., Deguchi, K., Himeno, M., Sato, M., Yamagiwa, H., Kimura, T., Yasui, N., *et al.* (1999) *Dev. Dyn.* **214,** 279–290.
17. Davis, A. P., Witte, D. P., Hsieh-Li, H. M., Potter, S. S. & Capecchi, M. R. (1995) *Nature* **375,** 791–795.
18. Kmita, M., Tarchini, B., Zakany, J., Logan, M., Tabin, C. J. & Duboule, D. (2005) *Nature* **435,** 1113–1116.
19. Boulet, A. M. & Capecchi, M. R. (2004) *Development (Cambridge, U.K.)* **131,** 299–309.
20. Vega, R. B., Matsuda, K., Oh, J., Barbosa, A. C., Yang, X., Meadows, E., McAnally, J., Pomajzl, C., Shelton, J. M., Richardson, J. A., *et al.* (2004) *Cell* **119,** 555–566.
21. Hill, T. P., Spater, D., Taketo, M. M., Birchmeier, W. & Hartmann, C. (2005) *Dev. Cell* **8,** 727–738.
22. Cosgrove, D., Gray, D., Dierich, A., Kaufman, J., Lemeur, M., Benoist, C. & Mathis, D. (1991) *Cell* **66,** 1051–1066.
23. Rodriguez, C. I., Buchholz, F., Galloway, J., Sequerra, R., Kasper, J., Ayala, R., Stewart, A. F. & Dymecki, S. M. (2000) *Nat. Genet.* **25,** 139–140.
24. Brown, S. D., Chambon, P., de Angelis, M. H. & Eumorphia Consortium (2005) *Nat. Genet.* **37,** 1155 (lett.).
25. Stricker, S., Fundele, R., Vortkamp, A. & Mundlos, S. (2002) *Dev. Biol.* **245,** 95–108.